

# Space Pollution metals contributing to Ozone Hole, South Atlantic Anomaly, and Radiation Belt

## Abstract

Since the 1970s, ozone (15–40 km) over Antarctica has continuously declined, which parallels the time of metallic satellites from the 1960s–2000s and discovery of Inner Radiation Belt (IRB). This is the first study to suggest heavy metals from satellites, debris, & rockets are correlated to Inner Radiation Belt (IRB), South Atlantic Anomaly (SAA) and Ozone hole and to propose the North Atlantic Anomaly (NAA). After high temperature corrosion (HTC) for <45 min sunward in Low Earth Orbit (up to 125C or 270F) and during re-entry, metals (Al, Fe, Mn, Ce, Pb) from satellites become ionized with high charges (+3, +2) and form metal oxides such as (Al<sub>2</sub>O<sub>3</sub>, Fe<sub>2</sub>O<sub>3</sub>, etc), metal hydroxides (Al(OH)<sub>n</sub>, Mn(OH)<sub>n</sub>, etc) until deposition as oxides, sulfides, and silicates. For example, after big reentry events such as 75-ton Skylab EDL fell to Earth in 1979, McConnell et al.,<sup>1</sup> recorded 40X increase in metals such as Al, Pb in ice in Antarctica with other studies finding Pb of 1000X+ and Cd of 10X+ in 1980s.

If SAA 3D Vortex and Radiation Belt co-located at ~200–500 km with trapped ionized particles and metals, heavy and light ion fluxes near poles would form metal oxides, ozone hole and reduce magnetic B-field, which may have formed largest ozone holes measured. Similar to how CFC atoms react with ozone, this study discusses how transition metals are a primary factor contributing to ozone depletion, metal oxides & silicates formation, observed in South America and Antarctica, which coincides with widespread desertification, extinctions, and warming. If metals from satellites in SAA deposit to poles with 2–16X heat absorption capacity to melt ice and radiation over poles, this could be a primary force melting ice in Polar Regions.

**Keywords:** space pollution, satellites, radiation belt, ozone, global warming

Volume 8 Issue 3 - 2024

**Kole Lutz**

Magneto Space, United States

**Correspondence:** Kole Lutz, Magneto Space, United States, Tel +17032448456, Email kole@magneto.space

**Received:** July 10, 2024 | **Published:** July 23, 2024

**Background:** The South Atlantic Anomaly (SAA) was discovered in 1958 and has led to several incidents with satellites and humans in orbit from 2000s–2020s from radiation, which is believed to be from trapped particles in SAA or Van Allen belt. Some suggest SAA is an indicator of a geomagnetic pole reversal, which occurs every ~780,000 years. Some research and data suggests current pole migration rate is too fast, far from values in Holocene and Brunhes eras. This mirrors heavy metals (Fe, Al, Mn, Pb, Tl, As) in Antarctica and south Atlantic that rose significantly during late 1900s. As satellites are a primary contributor to metals in stratosphere (12–50km), 10% of stratosphere large aerosol particles have metals (Al, Cu, Li, Lead, etc) which could grow from 10–50% by 2035–2040 (Figure 1).<sup>2</sup>

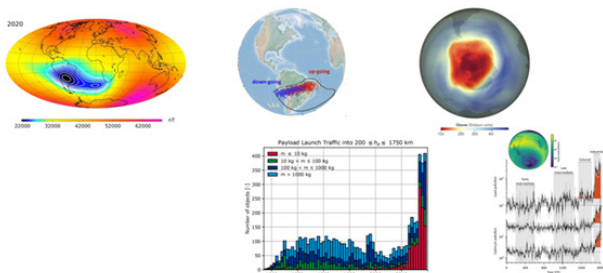


**Figure 1** a) South Atlantic anomaly b) Ions in SAA b) South Pole ozone hole (NASA, 2011) c) Satellites launched per year d) Heavy metal lead and Cd pollution.<sup>1</sup>

**Ozone hole:** Ozone reduced to 100 Dobson units and may appear to be radially skewed toward South America/Atlantic after 2002–2007 based on animation from by NASA’s Total Ozone Mapping Spectrometer (TOMS) instruments from NASA Earth Observatory, 2019. Chlorofluorocarbons (CFCs) long-lived chemicals that had

been used in refrigerators and aerosol sprays were believed to cause ozone depletion. Global recognition of CFCs led to the 1987 Montreal Protocol, a treaty phasing out the production of ozone-depleting chemicals. Since 1978, no aerosols made or sold in the U.S. have contained CFCs except for a tiny fraction (less than 2%). However, 30 years of ozone hole data from NASA TOMS, Aura Satellite and NOAA Suomi Satellite suggests CFC’s are not a contributing factor to ozone depletion. A 20% decrease in ozone depletion has also been observed during the winter months from 2005 to 2016. Similar to how CFC atoms are broken down and react with ozone molecules, this study proposes transition metals are the primary contributing factor causing ozone depletion.

## Takeaways

- i. South Atlantic Anomaly(SAA) causes significant losses in power (  $\delta P < 0$  ) generating capability—up to almost 8% and cause up to four years’ worth of ionizing dose degradation. SAA is believed to cause most SEU satellite failures and radiation to astronaut human health.
- ii. SAA or Inner Radiation Belt (IRB) is believed to be a swirling 3D vortex of metals and electron clouds electromagnetically trapped with (  $\nabla V_{ions} \sim 0$  ) spanning hundreds of km primarily from space pollution.
- iii. Research suggests Earth’s Magnetic Field (B<sub>x</sub>, B<sub>y</sub>) is not reversing and may be drifting at 0.23°S 0.34°W due to SAA and NAA, which may be correlated to metals from satellites and rockets.
- iv. How much radiation effects of astronauts, electronics failure from SAA/Van Allen belts?

v. What are ozone hole growth rates, similarities, & differences of North Atlantic Anomaly (NAA)?

**Introduction**

**South Atlantic anomaly (SAA)**

The SAA was discovered in 1958 with the southern boundary constant expanding northwest and north east<sup>3</sup> South Atlantic Anomaly (SAA) is estimated to be located at an altitude between 200 and 800 km (Figure 2).<sup>4</sup>

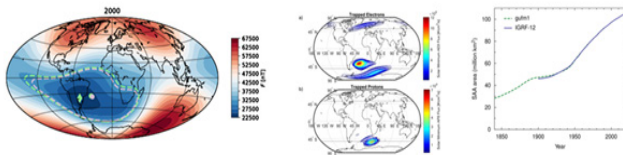


**Figure 2** a) SAA, b) Trapped particles in 400 km (Lenart, 2022) c) area of the magnetic field in the center of SAA.

**Effects of South Atlantic anomaly (SAA), radiation belts, and ionizing radiation in orbit**

SAA affects the radiation field in the atmosphere even down to the altitudes of civil aviation.<sup>5</sup> Satellites experience strong ionizing radiation over 4-8 minutes/orbit, which may be correlated and caused by the trapped particles in the inner Van Allen belt, located 200–1,000 km.<sup>6</sup> Biology is also effected in SAA as some astronauts mention seeing “shooting stars” (phosphenes), termed cosmic ray visual phenomena.<sup>7</sup> Passing through SAA caused many satellite failures with Globalstar network’s satellites in 2007.<sup>8</sup> The SAA destroyed Hitomi, Japan’s X-ray observatory after a series of events whereby SAA SEU disabled GNC subsystems onboard, which lost telemetry balance and then solar panels.<sup>9</sup>

Figure 3 outlines SEUs from ADEOS terminated unexpectedly in 2003 after passing through SAA in sun-synchronous,<sup>10</sup> sub-recurrent orbit (803-820 km) and an inclination of 98.7.<sup>11</sup> 200 keV with generally softer spectra than are normally found in the stable trapping region. In geomagnetic storms and solar maxima, electrons become trapped electromagnetically in IRB belts which increase by several orders of magnitude. In 2003, a geomagnetic storm with solar flares & CMEs caused 46 of the 70 satellite failures reported. The proton and heavy ion threat to spacecraft may also comes from GCRs and SEPES discrete components such as memories and transistors.<sup>12</sup> A worst-case event could lead to significant losses in power generating capability up to almost 8% and cause up to four years’ worth of ionizing dose degradation, leading to component damage and a life-shortening effect on satellites.<sup>13</sup>

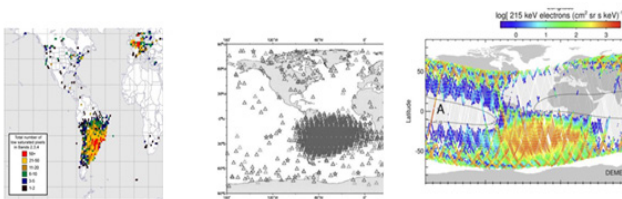


**Figure 3** a) single event upset (SEUs) from USGS Landsat satellite & failures of Swarm satellites in SAA 2014-2017,<sup>10</sup> b) SEUs from ADEOS Satellite failed in 2003,<sup>11</sup> c) Particles trapped, DEMETER satellite.

The areal extent of the SAA for 20 years from CHAOS-7.2 model monthly from 1998 to 2020.<sup>14</sup> With its center around 25 degrees South and 50 degrees West, the center was around 26.61°S 49.06°W and drifting at 0.23°S 0.34°W each year.<sup>15</sup> The SAA is estimated to be

located at an altitude between 200 and 800 km and ranges from –50° to 0° latitude and –90° to +40° longitude measured at 500km (Figure 4).<sup>16</sup>

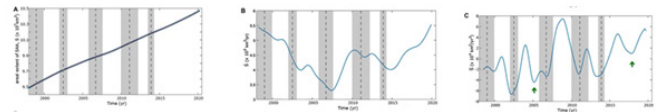


**Figure 4** South Atlantic Anomaly evolutions. (A) Evolution S, (B) first derivative S', and (C) second derivative S.

10 years of AMS-02 data on ISS identified ions below 5 GV in the SAA region. All stably-trapped ions have a pitch angle of about 90°. At centre of SAA, no ions were observed with small lifetime. A backtracking algorithm understands origin of a particle to reconstruct the particle’s trajectory in magnetic field (Figure 5).<sup>17</sup>

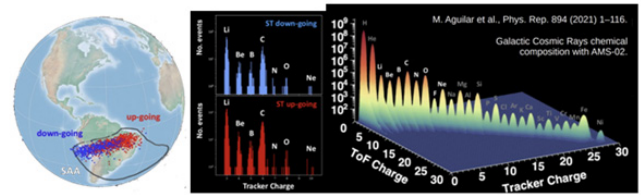


**Figure 5** a) down and upgoing ions, Heavy Nuclei Z>2 in SAA with AMS on ISS.<sup>17</sup>

**Inner radiation belts (IRB) correlated with South Atlantic anomaly and heavy ions**

Van Allen belts entail Particles trapped in the Earth’s magnetic field with high radiation close to surface at the South Atlantic Anomaly.<sup>18,19</sup> Inner Radiation Belts (IRB) dips to 200 km. The flux doses inside of the ISS vary in the range 74–215 µGy/d–1 per day for and 130–258 µSv/d–1 for the averaged equivalent daily dose rates. This reduces atmosphere ppm and high photon flux and dose rate in SAA<sup>20</sup> and drives metal oxide formation, reducing EM field.

**Heavy metals deposited from stratosphere from space systems and reentry**

20+ metals (Cu, Li, Al, and lead) 10% of aerosol particles in stratosphere contain metals. In addition to these two unusual elements, a significant number of particles contained metals such as copper, lithium and aluminum. Particles with metal could grow from 10-50% by 2035-2040 (Figure 6).<sup>21</sup> At 360 tonnes of aluminum oxide (Al<sub>2</sub>O<sub>3</sub>) particles in the atmosphere each year, 30 kilograms (66lbs) of aluminum oxides are produced by the burning of a 250-kilogram satellite. In 2022, 17 tonnes of aluminum oxide nanoparticles were released into the atmosphere from satellites. In February 2024, SpaceX announced controlled descent of 100 older (227kg) Starlink satellites (which have 5 - 7 year lifespan) into lower orbits over the next six months due to design flaw.

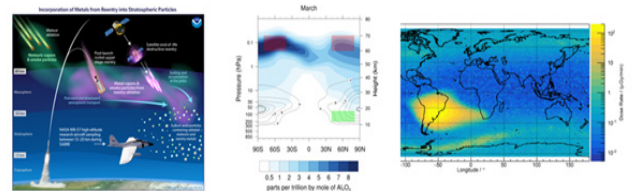


**Figure 6** Metals from Reentry, monthly Al<sub>2</sub>O<sub>3</sub> from reentry for the 15yr simulation.<sup>21</sup> Dose rate (µGy/min) in silicon at 600 km from the DLR CROPIS satellite in Mar/Apr 2021.<sup>5</sup>

Satellite industry is based on 60 years with tin-lead solder joints. Figure 6 b) outlines contours with mass mixing ratio and the contour lines show the mass density in 10–16 g cm<sup>-3</sup> with bold contour 2.4 × 10–16 g cm<sup>-3</sup>. In figure 6c, Silicon is used in many parts of satellites, including their structure, wafers, electronics, and solar panels. Most common silicon-based material is Polydimethylsiloxane (PDMS) resins, which are used in large amounts on satellites with structure CH<sub>3</sub>[Si(CH<sub>3</sub>)<sub>2</sub>O]<sub>n</sub>Si(CH<sub>3</sub>)<sub>3</sub>.

### Heavy metal concentrations in Antarctica and South Atlantic

With 100X+ increase in Pb, 10X+ increase in Cd, aluminosilicate ( Si-O-Al<sub>2</sub>SiO<sub>3</sub> ) dust deposition increased by 2X in late 1900s, which parallels ≈1°C Southern Hemisphere and drove vast desertification around Patagonia and northern Argentina. (Figure 7).<sup>1</sup>

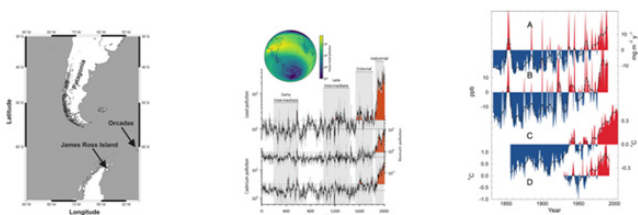


**Figure 7** Patagonia and James Ross b) Metals in South Atlantic, c) aluminosilicate dust levels (B) at James Ross Island, and Southern Hemisphere (C) and southern Patagonian (D) air temperatures.<sup>1</sup>

Lead pollution in Antarctica spiked in the 1900s. In 1975, catalytic converters were in and lead was out. Leaded gasoline: practice was phased out in the 1990s by government regulations, but the lead from leaded gasoline is still present in soil and dust. Moreover, lead is used in the tin-lead (Sn-Pb) solder for all electronics used in space for 60 years contributing tin-lead to Earth’s environment. As of 2020’s NASA requires the use of Sn-Pb solder and part surface finishes with a minimum of 3% lead (Figure 8).<sup>22</sup>

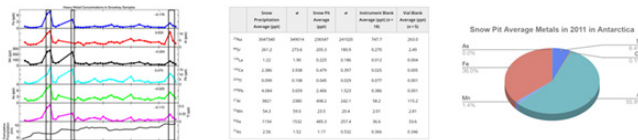


**Figure 8** Heavy metals in 310 samples (160 snow precip, 150 snow pit samples) in Roosevelt Island.<sup>22</sup>

On September 24, NASA’s Upper Atmosphere Research Satellite, or UARS, re-entered Earth’s atmosphere and crashed in the Pacific Ocean. 5900kg UARS was made of aluminum alloy 6061 or 7075, was the largest NASA satellite to re-enter in 30 years, ironically also collecting data on ozone, CFC’s. Operational altitude of 600 kilometers. Operations Center for JFCC-Space tracked the vast majority of the orbital transit was over water, with some flight over northern Canada and West Africa. Surviving components would be 57 degrees north latitude and 57 degrees south latitude.<sup>23</sup> UARS separated into 26 pieces, (10-300lbs) with some of stainless steel, titanium and beryllium that have very high melting temperatures.

Tuohy 2015 et al.,<sup>22</sup> measures Pb, Tl, Al, Mn, As, and Fe in surface snow samples collected over 70 days with spikes of with 59% Al, 36% Fe and 6.4% Strontium, known to block X-rays denoted in Figure 8c chart. Based on data from Figure 8b, Boxes indicate days when fog persisted all day accompanied by extensive rime ice growth. Snow pit heavy metals peak in late November to early December. If metal samples and anomalies correlated with UARS, this would suggest

metal atmosphere transit duration of 36-48 days + until surface deposition for of a % of satellite materials corroded from UARS. Further research would help quantify mean free path of metals and potential correlation with South Atlantic Anomaly (SAA). Other events may be analyzed such as 75-ton Skylab that scattered debris across the Indian Ocean and Western Australia and fell back to Earth in July 1979.

75 ton Skylab reentry was monitored from Air Force tracking system.<sup>24</sup> Debris from station had separated at 10 miles above the Earth into several pieces. Shortly after 75-ton Skylab re-entered in 1979, a 40X increase in Aluminum at James Ross Antarctica, Patagonia, and Southern Hemisphere was measured alongside increase in air temperatures (D) highlighted in Figure 9. A separate study found detailed measurements of the toxic heavy metals lead, cadmium, and thallium in East Antarctic ice cores increased by orders of magnitude in late 1900s. Moreover, researchers measured it would take <30 years for aluminum oxides to drift down to stratospheric altitudes, which contains 90% of Earth’s ozone.<sup>25</sup> However, previous models do not factored in high ionization charge states, radiation belt dynamics, and electromagnetic fields on ion trajectories (Figure 10).

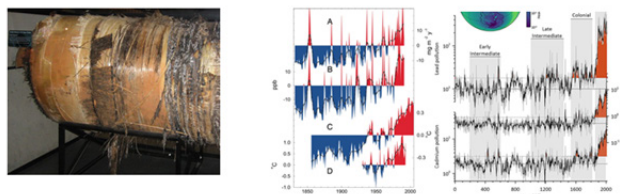


**Figure 9** a) 75ton Skylab after EDL in 1979 b) & c) Metals and Al in Antarctica & South Atlantic.<sup>1</sup>

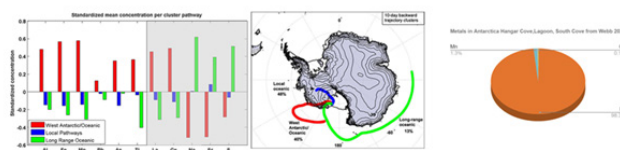


**Figure 10** HySPLIT clustered air mass pathways calculated from 123 back trajectories from summer 2011 to 2012. Topographic data are from Timmerman et al.,<sup>22</sup>

In West Antarctica, The highest amount of metals in samples over summer is associated with air masses columns. Moreover, V, Cr, Mn, Cu, Zn, Co, Ag, Cd, Ba, Pb, Bi and U were detected in snow samples from 1834 to 1990, from low accumulation sites in Coats Land, Antarctica. This may be correlated to Non-ferrous metal mining and smelting emissions in Chile, Peru, Zaire, Zambia and Australia.<sup>26</sup> In Antarctica at Lake Vanda (Wright Valley), significant increases in metal concentrations begin to appear at depth, between 57 and 60m. Vertical profiles suggest that the entire suite of trace metals dissolved and particulate Mn, Fe, Ni, Cu, Zn and Cd in the water column.<sup>27</sup> With highest ppm of Manganese (Mn) and Iron (Fe) alloys, stainless steels grades such as 316 are around 62% iron, 16-18% Chromium, 10–14% nickel, 2–3% molybdenum, and traces of others. Cu is also widely used in circuit PCB boards and electronics in satellites.

In three species of invertebrates Laternula elliptica (mud clam, filter feeder), Nacella concinna (limpet, grazer) and Odontaster validus (seastar, predator and scavenger), Nine metals (Cd, Co, Cr, Cu, Fe, Mn, Ni, Pb, Zn) were detected. Sediment samples from Hangar Cove, South Cove and Lagoon Island all had a grain size of (62.5µm) 0.063–0.1 mm. Comparing sediments collected for this study in 2011 was similar to 2006. Laternula elliptica clams had mean shell length was 62.5 mm. Bedrock metals were from glacial activity (Figure 11).<sup>28</sup>

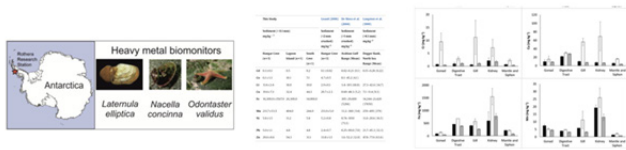


**Figure 11** a) Metal in Rothera Research Station on west Antarctic Peninsula b) and c) Metal concentrations in five soft tissues (gonad, digestive tract, gill, kidney, and mantle and siphon) from *L. elliptica* Clams.<sup>28</sup>

Perryman 2020 et al.,<sup>29</sup> found high concentrations of heavy metals are distributed in soils across Alaska. In analyzing 1000 samples, five metals: arsenic, chromium, lead, mercury, and nickel, and found that concentrations were 10X higher than the average for US soils. Cr, He, and Pb were higher in soils below 10 cm depth. Study investigates how metals thaw permafrost soils and become mobilized, with higher risk for Arctic communities.

Publications on heavy metals in Antarctica from 2000 to 2020 are reviewed and have increased to 106 documents indicated from Scopus.<sup>30</sup> Microbes on metals in Antarctica may be used as biosensors to detect metals in environments. Studies on Antarctic microorganisms cite several accounts of bioremediation of metal pollution. Manganese-reducing organisms are active in zone of metal release Bratina et al.,<sup>31</sup> Glatstein et al.,<sup>32</sup> found bioremediation of As and Cd with 4 *Pseudomonas* sp. strains from Antarctica. Many strains biosynthesize cadmium sulfide (CdS). Metals in aquatic ecosystems are a significant threat to human and animal health. Constants of Solubility of Metal Hydroxides and of Solubility Products of Metal Sulfides are outlined from.<sup>33</sup>

**Ozone layer depletion in South and North Pole**

Ozone depletion over the North Pole, leads to the formation of polar stratospheric clouds (PSCs) and high-altitude clouds, which trap cold air in polar vortex with recorded measurements available from in 2010-2011 and 2020 (Figure 12). In 2020, Ozone hole three times the size of Greenland was discovered over the North Pole.<sup>34</sup> However some researchers such as EU’s Copernicus Atmosphere Monitoring Service (CAMS) believe the ozone hole closed low magnetic field in the South Atlantic Anomaly (SAA) zone facilitates the entrance of high-energy particles from the magnetosphere. Effects over the total column ozone (TCO), NOx (=NO+NO2) and ozone profiles in the SAA zone during and after two intense geomagnetic storms during solar cycle 23 are analyzed.<sup>35</sup>

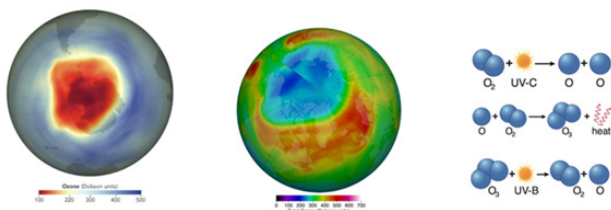


**Figure 12** a) Ozone depletion in South Pole from Oct, 2011 NASA Earth Observatory, 2019 b) North Pole Arctic stratospheric ozone reached record low of 205 Dobsons in 2020.<sup>18</sup>

**GeoMagnetic field pole drifting**

Some studies associate magnetic field drifting anomaly as a precursor for a geomagnetic transition, or reversal. Reversal potential correlation was suggested based on statistical calculations, if EM field is reversed every 400,000 years on average and last reversal occurred 780,000 years ago (Figure 13 & 14).<sup>36</sup>

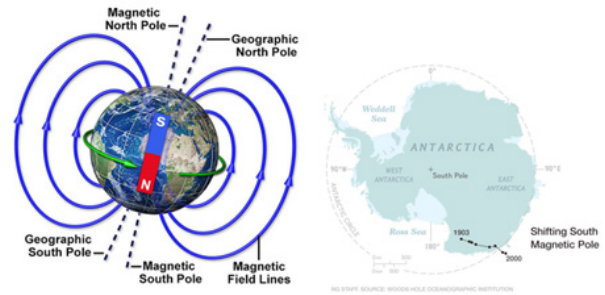


**Figure 13** Geomagnetic South Pole field drift.

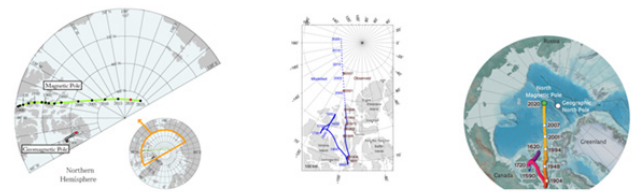


**Figure 14** Geomagnetic North Pole field drift.

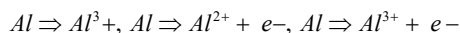
By sampling and analyzing paleomagnetic data from sediment cores and volcanic rocks from 50,000 to 30,000 years before present, low intensity areas measured did not lead to a reversal of the poles. Based on observations of the past 50,000 years we conclude that the SAA does not correlate reversal of the poles.<sup>10</sup> The SAA is likely not associated with a geomagnetic reversal, because the present value seems to be different with DM during the Holocene (last 12 ka) and Brunhes polarity chron (last 0.78 ka).

The global model SHA.DIF.14k was compared with Holocene.<sup>37</sup> CMB Magnetic pole under the South Atlantic Ocean is growing at rate of  $-2.54 \cdot 10^5$  nT per 100 years associated with western drift. Dipolar moment ( $7.7 \cdot 10^{22} \text{A} \cdot \text{m}^2$ ) is not as low based on paleomagnetic data for Holocene (last 12 ka) and Brunhes geomagnetic normal polarity (last ~0.8 Ma).<sup>36</sup> During Holocene dipole moment (DM) oscillated from 4 and  $11 \times 10^{22} \text{A} \cdot \text{m}^2$  with average of  $8.1 \pm 1.6 \times 10^{22} \text{A} \cdot \text{m}^2$ . The current field drift is decreasing at  $-12\%$  per 100 years, faster than expected for EM field polar transition.<sup>38</sup> World magnetic model (WMM) contains five magnetic zones and is utilized for navigation, attitude, and heading. Operated from US National Geophysical Data Center (NGDC), WMM is adjusted every 5 years and guides military and commercial aviation routes. The geo magnetic field is important for biological systems including birds, and other animals both land and marine that depend on magnetoreceptor sensors for migration and survival.

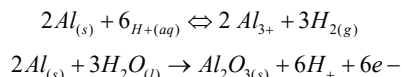
**Methods**

**Metal oxide reaction pathways in atmosphere and ground**

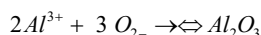
With eV flux of oxygen in LEO <2000km and  $-65 \text{ }^\circ\text{C}$  to  $+125 \text{ }^\circ\text{C}$  (270F) in orbit, high temperature corrosion (HTC) of aluminum and solar panels per 90-120 min period and during reentry oxidizes and scatters surface metals. Al oxides have increased 8-fold between 2016 and 2022 and will continue to accumulate as the number of low-Earth-orbit satellites. With 50,000 satellites with starlink, 10,000 per year re-entering, a 646% increase of Al oxide above natural atmospheric levels.<sup>25</sup>



Aluminum has three oxidation states. The most common one is +3. The other two are +1 and +2. Electron configuration for Aluminum is 1s22s22p63s23p1.



Aluminum oxide is generally less reactive as Al<sup>3+</sup> ions and O<sub>2</sub><sup>-</sup> form an ionic lattice that is stable in cubic structure with ions occupying small octahedral holes.



With high levels of Aluminosilicate MAIO<sub>2</sub>(SiO<sub>2</sub>)<sub>x</sub>(H<sub>2</sub>O)<sub>y</sub> where M<sup>+</sup> is usually H<sup>+</sup> and Na<sup>+</sup>, earth's crust chemical composition is rich in silica and alumina (about 59% of SiO<sub>2</sub> and 16% of Al<sub>2</sub>O<sub>3</sub> in the outermost 20 km).



Hydroxyaluminosilicates (HAS) is crucial in the non-selection of aluminum in biochemical evolution and in combating the ecotoxicity of aluminum including exposure to aluminum.<sup>39</sup>

Volcanoes are a natural source of sulfur oxides, a highly reactive gas, in the atmosphere, however, close to 99% of the sulfur dioxide (SO<sub>2</sub>) in the atmosphere comes from human activity. Gaseous SO<sub>x</sub> can harm trees and plants by damaging foliage and decreasing growth. UV sunlight and H<sub>2</sub>O in the high atmosphere can convert sulfur dioxide into sulfuric acid clouds. With metal coexistence and affinity toward sulfur-based compounds, sulfides may form from direct combination of metals with sulfur by the reduction of sulfate (Figure 15).

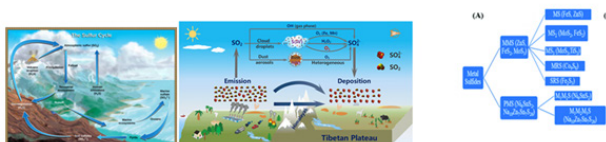


Figure 15 a) Sulfur cycle b) SO<sub>2</sub> to SO<sub>4</sub> pathways c) Metal sulfide pathways.<sup>40</sup>

Another source of sulfur may be from exhaust of aerospace rockets which consists of CO<sub>2</sub>, H<sub>2</sub>O vapor, soot, nitrous oxides, and sulfur. Potential coexistence with sulfuric acid particles as H<sub>2</sub>SO<sub>4</sub>, this would suggest -2 charge donates H<sup>+</sup> to metals and sulphuric acid reacts with metals to produce sulfur dioxide (SO<sub>2</sub>), which would produce H<sub>2</sub> gas and salts. Metal sulfates such as Aluminum sulfate, Al<sub>2</sub>(SO<sub>4</sub>)<sub>3</sub>•18H<sub>2</sub>O, LiSO<sub>4</sub>, CuSO<sub>4</sub> may also be formed from oxide and sulfuric acid. Moreover, Aqueous Adsorption of Heavy Metals on Metal Sulfide Nanomaterials is outlined from<sup>40</sup> that suggest metal sulfides are a remediation technology to adsorb metals (Figure 16).

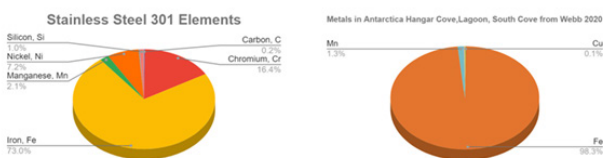


Figure 16 Stainless Steel elements and metals in Antarctica from Webb 2020.<sup>28</sup>

301 Stainless Steel is found in automobile molding and trim, wheel cover, conveyor belts, kitchen equipment, roof draining systems, hose clamps, springs, truck and trailer bodies, railway and subway cars.

SpaceX Starship transitioned to 301 and 304 stainless steels. Falcon 9 Block 6 has a stainless steel center core. If stainless Grade 310 UNS S31000 is also common, this material has 24-26% Cr, 19-22% Ni, 2X higher concentrations of Cr and Ni than steel 301 with 2% Mn. Some steels are alloyed that contains between 2-14% manganese. With metal Thermal conductivity ranges (ability to maintain heat transfer), Stainless steel is 14 W/m K outperforms Aluminum at 240 W/m K and Manganese at 7 W/m K and Fe around 35 W/mK around 1832°F (Figure 17).

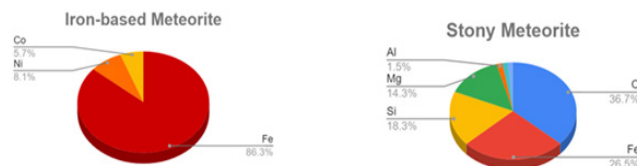


Figure 17 Fe and stony meteorite composition.

C-type (chondrite) asteroids are most common primarily made of clay and silicate rocks. The S-types (stony) are made up of silicate materials and nickel-iron. Asteroids such as carbonaceous, enstatite, and ordinary chondrites: also contain significant amounts of copper, around 70-100 parts per million (ppm) by mass (Figure 18).<sup>41</sup>

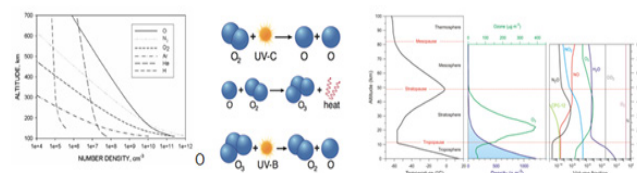
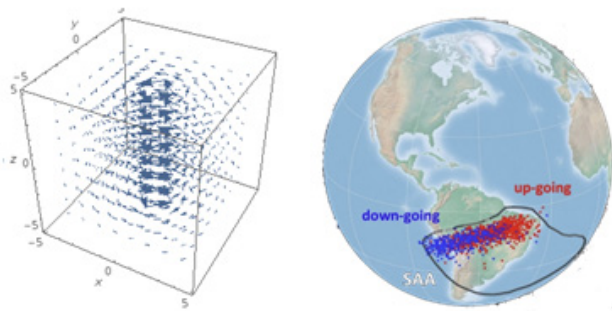


Figure 18 a) Atmospheric vs altitude b) Atomic Oxygen (AO) Pathways, c) Generalic<sup>41</sup>

The SAA altitude range of 200-500 to 800km+ suggests metal oxides form and react with O, O<sub>2</sub>, and O<sub>3</sub>, where they become heavier and denser. To find out where metal such as mercury would land after reentry, Pirrone used an atmospheric-transport model to simulate how the heavy metal would fall to Earth's surface. Around 75 percent of the spent fuel from satellites would deposit in the oceans, factoring in wind patterns and other atmospheric processes. Moreover, mercury ions released at 40-50 km s<sup>-1</sup> at 1000 km altitude in a polar orbit are effectively constrained to spiraling back and forth between the polar magnetic mirror points (where charged particles trapped in the Earth's magnetic field reverse their direction). Roughly half of the ion trajectories have mirror points at altitudes below 100 km.<sup>42</sup> Moreover, 1/3 of xenon ion trajectories released at 44 km s<sup>-1</sup> at altitudes from 15,000 to 115,000 km were retained in a stable orbit over a 2-7 week simulation period, remaining in atmosphere and orbit.<sup>43</sup> However, previous models have not factored in the high ionization charge states, van Allen radiation belt dynamics, and electromagnetic field intensities on ion trajectories. Research suggests that after forming metal oxides, metals would have greater density and probability of falling to local wind currents somewhere around 80-200 km with Karman line at 100 km altitude (Figure 19).

Ion Mean free path can be modeled and adapted based on.<sup>42</sup> To model collocation of ions and metal distribution in SAA, IRB radiation belt, and Ozone layers, vortex models can be adapted from:

$$\Delta V(x, y, z) = \left\langle -\frac{y}{x^2 + y^2}, \frac{x}{x^2 + y^2} \right\rangle$$



**Figure 19** a) Vortex Curl from WolframAlpha b) Up and down ions in South Atlantic Anomaly (SAA).

Curl is a measure of how much vector field circulates where irrotational vortices models would help to factor in turbulence, chemical reaction pathways, electromagnetic interactions, and wind models. Tangential component of the particle velocity could model stability, ion trajectory, and particle lifespan in atmosphere.

Research suggests the South Atlantic Anomaly is a massive 100-500km+ cloud of ionized metal and electrons electromagnetically bound in microgravity. With metal-based sub cloud clusters, metals would react with atomic oxygen and oxygen to form denser metal oxides, which would fall and cluster at higher ppm in lower altitudes. If higher charge states in inner cloud clusters, imaging, signals, and systems may interact with ionized metals such as  $Fe^{3/2+}$ ,  $Al^{3/2+}$ ,  $Mn^{3/2+}$  which would have shorter radius and different ion trajectory velocities. During solar maximum, highest metal oxides, ionized ions, and plasma charge density would create high irrotational vortices and electromagnetic turbulence with pressure gradients. Further research will help quantify updraft and downdraft pressure forces, fluxes, particles species, in South (SAA) and North Atlantic Anomalies (NAA).

### Metal nanoparticle atomic size analysis & comparison

Nanoparticle Atomic Sizes can distinguish which particles would be from cars and which from satellites and reentry, from higher up in atmosphere. Particle active surface emitted by newer vehicles is on average 3X higher. Around 50% of examined vehicles with low mileage in Russia emitted particles with diameter  $>10 \mu m$ . Captured from Exhaust Gas Suspension (EGS), the exhaust gas particulate categorized into three size classes: (1) 0.1–5  $\mu m$  – soot and ash particles, metals (Au, Pt, Pd, Ir); (2) 10–30  $\mu m$  – metal (Cr, Fe, Cu, Zr, Ni) and ash particles; (3) 400–1,000  $\mu m$  – metal (Fe, Cr, Pb) and ash particles. The above particle classes are divided approximately as follows: (1) 10–15%, (2) 65–70%, (3) 15–25%.<sup>44</sup> Newer vehicles with low mileage are substantial sources of soot and metal particles with median diameter of 200 nm with a higher surface area (up to 89,871.16  $cm^2/cm^3$ ). This suggests, 10–30  $\mu m$  – metal (Cr, Fe, Cu, Zr, Ni) are related to direct fuel combustion products related to nonlinear corrosion dynamics and surface reactions at high temperatures of local manufactured exhaust tailpipes. This would further suggest that exhaust emitted metals would have different atomic size than metal nanoparticles.

### Discussion

Future research aims to quantify the specific heat capacity of metals vs  $CO_2$  and  $CH_4$  on polar ice melt rates. A high value of specific heat suggests more energy to raise or lower temperature whereby lower values suggest less energy heat. In addition to increased radiation flux over poles from ozone hole, research suggests heavy

metals such as Al, Fe, Steel, Cr, Cu, Mercury, Gold, and Lead with specific heat capacity ranges of (128-500 J/kg/C) vs  $CO_2$  (839 J/kg/c), water at (4,186 J/kg/C and Ice at 2093 J/kg/C heat up atmosphere and accelerate melting of ice. Mercury, Gold, Lead, and other metals 600% more effective at absorbing heat and inducing greenhouse effect than  $CO_2$ .

### Systems and solutions to neutralize Atlantic anomaly, plasma clouds, & radiation belt

To neutralize plasma clouds and high ionized particles, Lutz K, Trevino T 2024 et al.,<sup>45</sup> outline High energy laser & systems to neutralize stellar coronal mass ejections (CME) plasma. As high-FIP atoms are electromagnetically trapped with a higher susceptibility from lower e- density and temperatures, CME plasma clouds can be neutralized, separated, and reduced in velocity trajectory. Less invasive approach holds potential to separate electromagnetic forces between ion clusters, fill valence e-, and polarize CME column charge densities, with optimal CME scatter geometry and time window. Metal sulfide materials are a promising strategy due to their cost-effective, environmentally friendly, surface modulational, and amenable properties.

However, previous methods involved more invasive measures in contaminated waters. Novel systems such as Electromagnetic plates could attract and form, generate, and capture metal oxides to fill oxygen gaps. Deposition of elements near vicinity of SAA and NAA may be released near up and down ion movement on day and/or night side across km altitudes. Other materials such as wood and other less reactive metals provide good structural material with radiation resistance and low thermal conductivity. Satellite manufacturers, operators, space agencies and industry may discuss a treaty agreement similar to Montreal 1987 Protocol which banned use of CFCs, on contributing to space pollution heavy metals.

### Questions

- How much variance of geomagnetic poles is there during solar storms and solar peak?
- How do arctic wind currents and climate affect metal trajectory and deposition?
- What are ozone hole growth rates, similarities and differences of such a North Atlantic Anomaly (NAA)?
- How to quantify whether geomagnetic pole drift is correlated with SAA and NAA?

### Future research and experiments

Instruments measure daily metal sedimentation rate at sites and Geochemistry formation such as aluminosilicate  $(MAIO_2)(SiO_2)_x(H_2O)_y$  where  $M^+$  is usually  $H^+$  and  $Na^+$ , (zeolites) that are synthesized by reactions of silicates, aluminates, and other compounds. Measure other metal-silicate concentrations and compare with data. To measure particle size distribution, laser particle size analyzer may be supplied with Fritch MaS software, XRD with PM morphology by SEM and energy dispersive spectrometer. A high resolution, inductively-coupled plasma mass spectrometer may measure metals in collected liquid samples stored at 4C. Snow Pit Sampling Methods based on Tuohy A et al.<sup>22,44</sup>

### Future research and experiments will:

- Image ion trajectory, and particle lifespan of SAA and NAA in atmosphere correlated with ozone hole and heavy metal corrosion from satellites and rockets.

- ii. Measure metal particle diameter of heavy metals deposited near poles and SAA and compare with metal diameter and metal properties from vehicle exhaust emissions.
- iii. Quantify effects of metals on photosynthetic plants, algae, and uptake enzyme pathways alongside widespread desertification in South America such as Patagonia and Argentina.
- iv. Ground and space-based instruments and missions to image HTC metal trajectory and contribution to IRB radiation belts and SAA from rockets.
- v. Correlate and analyze effects on, ice melting, and electromagnetic field stability of planet.

## Acknowledgments

None.

## Conflicts of interest

The authors declare that there is no conflict of interest.

## References

1. McConnell JR, Aristarain AJ, Ryan Banta J, et al. 20th-Century doubling in dust archived in an Antarctic Peninsula ice core parallels climate change and desertification in South America. *Environmental sciences*. 2007;104(14):5743–5748.
2. NASA/GSFC. The Van Allen Belts. 2019.
3. Broad WJ. Dip on earth is big trouble in space. *The New York Times*; 1990.
4. Lenart A, Sivasankaran S, Hidding B, et al. CubeSat in-orbit validation of in-situ performance by high fidelity radiation modelling. *Nature portfolio*. 2022.
5. Meier MM, Berger T, Jahn T, et al. Impact of the South Atlantic Anomaly on radiation exposure at flight altitudes during solar minimum. *Sci Rep*. 2023;13:9348.
6. Walt M. Introduction to Geomagnetically trapped radiation. Cambridge, New York: Cambridge University Press; 1994.
7. Sten O. What is the South Atlantic Anomaly? In: *Ask the Astronomer*. CreateSpace Independent Publishing Platform; 2015.
8. Todd. Space Intelligence News; 2007.
9. Moon M. Japan's most powerful X-ray satellite is dead. *Engadget*. 2016.
10. Brown M, Korte M, Holme R, et al. Earth's magnetic field is probably not reversing. *Earth, atmospheric, and planetary sciences*. 2018;115(20):5111–5116.
11. Kimoto Y, Nemoto N, Matsumoto H, et al. Space radiation environment and its effects on satellites: Analysis of the first data from TEDA on board ADEOS-II. *IEEE Transactions on Nuclear Science*. 2005;52:1574–1578.
12. Maurer RH, Fretz K, Angert MP, et al. Radiation induced single event effects on the Van Allen Probes spacecraft. *IEEE Transactions on Nuclear Science*. 2017;1(11):2782–2793.
13. Hands ADP, Ryden KA, Meredith NP, et al. Radiation effects on satellites during extreme space weather events. *Space Weather*. 2018;16:1216–1226.
14. Campuzano SA, Pavón-Carrasco FJ, De Santis A, et al. South Atlantic anomaly areal extent as a possible indicator of geomagnetic jerks in the satellite era. *Front Earth Sci*. 2020;8.
15. Kovář P, Sommer M. CubeSat observation of the radiation field of the south Atlantic anomaly. *Remote Sensing*. 2021;13(7): 1274.
16. GSFC. The South Atlantic Anomaly, Ask an Astrophysicist. NASA; 1996.
17. Valencia O. Properties of heavy nuclei in South Atlantic Anomaly with AMS-02. The 27th European Cosmic Ray Symposium; Netherlands: 2022.
18. Gray E. NASA reports arctic stratospheric ozone depletion hit record low in March. NASA SGFC, NASA's Earth Science News Team. 2020.
19. Underwood C, Brock DJ, Williams PS, et al. Radiation environment measurements with the cosmic ray experiments on-board the KITSAT-1 and PoSAT-1 Micro-Satellites. *IEEE Transactions on Nuclear Science*. 1994;41(6):2353–2360.
20. Dachev P, Tomov BT, Matviichuk YN, et al. Solar cycle variations of MIR radiation environment as observed by the LIULIN dosimeter. *Radiation measurements*. 1999;30(3):269–274.
21. Murphy DM. Metals from spacecraft reentry in stratospheric aerosol particles. *Earth, atmospheric, and planetary sciences*. 2023;120(43):e2313374120.
22. Tuohy A, Bertler N, Neff P, et al. Transport and deposition of heavy metals in the Ross Sea Region, Antarctica. *J Geophys Res Atmos*. 2015;120(10):996–1101.
23. NASA's UARS re-enters earth's atmosphere. *SpaceNews*; 2011.
24. Don L. Lind oral history transcript. Space Center Oral History Project, NASA Johnson; 2005.
25. Ferreira JP, Huang Z, Nomura K, et al. Potential ozone depletion from satellite demise during atmospheric reentry in the era of mega-constellations. *Geophysical Research Letters*. 2024;51(11):e2024GL109280.
26. Frédéric AM, Boutron CF, Barbante C, et al. Changes in heavy metals in Antarctic snow from Coats Land since the mid-19th to the late-20th century. *Earth and Planetary Science Letters*. 2002;200(1–2):207–222.
27. Green WJ, Stage BR, Bratina BJ, et al. Nickel, Copper, Zinc and Cadmium cycling with manganese in lake vanda (Wright Valley, Antarctica). *Aquat Geochem*. 2004;10:303–323.
28. Webb AL, Hughes KA, Grand MM, et al. Sources of elevated heavy metal concentrations in sediments and benthic marine invertebrates of the western Antarctic Peninsula. *Science of The Total Environment*. 2020;698.
29. Perryman CR, Wirsing J, Bennett KA, et al. Heavy metals in the Arctic: distribution and enrichment of five metals in Alaskan soils. *PLOS ONE* 2020;15(6):e0233297.
30. Darham S, Zakaria NN, Zulkharnain A, et al. Antarctic heavy metal pollution and remediation efforts: state of the art of research and scientific publications. *Brazilian journal of microbiology*. 2023;54(3):2011–2026.
31. Bratina BJ, Stevenson BS, Green WJ, et al. Manganese reduction by microbes from the oxic regions of the lake vanda (Antarctica) water column. *Appl Environ Microbiol*. 1998;64:3791–3797.
32. Glatstein DA, Bruna N, Benavente CG, et al. Arsenic and cadmium bioremediation by Antarctic bacteria capable of biosynthesizing CdS fluorescent nanoparticles. *J Environ Eng*. 2018;144:04017107.
33. Blais J, et al. Metals precipitation from effluents: review. *Practice Periodical of Hazardous, Toxic, and Radioactive Waste Management*. 2008;12:3.
34. Spektor B. Ozone hole three times the size of Greenland opens over the North Pole. *Livescience*. 2020.
35. Zossi MM, Zotto EM, Mansilla GA. Can geomagnetic storms affect stratospheric O<sub>3</sub> and NO<sub>x</sub> in the South Atlantic Anomaly Zone? *Pure Appl Geophys*. 2021;178:141–154.
36. Carrasco FJP, De Santis A. The South Atlantic Anomaly: the key for a possible geomagnetic reversal. *Frontiers in Earth Science*. 2016;4.

37. Pavón-Carrasco FJ, Osete ML, Torta JM, et al. A geomagnetic field model for the Holocene based on archaeomagnetic and lava flow data. *Earth Planet Sci Lett.* 2014;388:98–109.
38. Laj C, Kissel C. An impending geomagnetic transition? Hints from the past. *Front Earth Sci.* 2015;3:61.
39. Exley C. Darwin, natural selection and the biological essentiality of aluminum and silicon. *Trends Biochem Sci.* 2009;34:589–593.
40. Kromah V, Zhang G. Aqueous adsorption of heavy metals on metal sulfide nanomaterials: synthesis and application. *Water.* 2021;13(13):1843.
41. Generalic Eni. Atmosphere, Croatian-English chemistry dictionary & glossary. 2022.
42. Fourie D, Hedgecock IM, De Simone F, et al. Are mercury emissions from satellite electric propulsion an environmental concern? *Environmental Research Letters.* 2019;14(12).
43. Crofton MW, Hain TD. Environmental considerations for xenon electric propulsion. 30th Int Electric Propulsion Conf; Florence, Italy: 2007 September 17–20.
44. Golokhvast KS, Chernyshev VV, Chaika VV, et al. Size-segregated emissions and metal content of vehicle-emitted particles as a function of mileage: Implications to population exposure. *Environmental research.* 2015;142:479–485.
45. Lutz K, Trevino T. High energy laser & systems to neutralise stellar coronal mass ejections (CME) plasma. *Aeron Aero Open Access J.* 2024;8(1):1-9.